An Attractor-based Whole-Body Motion Control (WBMC) System for Humanoid Robots

Federico L. Moro[1], Michael Gienger[2], Ambarish Goswami[3], Nikos G. Tsagarakis[1] and Darwin G. Caldwell[1]

***Abstract*— This paper presents a novel whole-body torque-control concept for humanoid walking robots. The presented Whole-Body Motion Control (WBMC) system combines several unique concepts. First, a computationally efficient gravity compensation algorithm for floating-base systems is derived. Second, a novel balancing approach is proposed, which exploits a set of fundamental physical principles from rigid multi-body dynamics, such as the overall linear and angular momentum, and a minimum effort formulation. Third, a set of *attractors* is used to implement movement features such as to avoid joint limits or to create end-effector movements. Superposing several of these attractors allows to generate complex whole-body movements to perform different tasks simultaneously. The modular structure of the proposed control system easily allows extensions. The presented concepts have been validated both in simulations, and on the 29-dofs compliant torque-controlled humanoid robot COMAN. The WBMC has proven robust to the unavoidable model errors.**

I. Introduction

With growing research interest in humanoid robotics in recent years, robots have become increasingly proficient in performing many different, non-trivial tasks, such as running, jumping, climbing stairs, and manipulating objects. In most cases, however, each of these tasks is addressed individually, and this imposes a fundamental limitation on the use of humanoids in the real world. While humans may be outperformed by robots in a single task, they are vastly more capable of adapting and combining behaviors to solve different tasks. This flexibility allows humans to generalize their knowledge, and successfully perform tasks that they have never faced before. This also opens the door for simultaneous execution of multiple tasks [1][2].

To address these constraints, the class of whole-body control systems is a promising research direction. They represent a wide range of complex movement skills in form of low-dimensional task descriptors which are projected on the robot's actuators, such exploiting the full capabilities of the entire body. The literature in this area is vast, and two main directions have emerged. Inverse kinematics concepts utilize kinematic redundancy resolution [3][4][5], and are particularly popular due to their compatibility with velocity-controlled robots. More recently, torque-controlled humanoid robots have become available. Control concepts based on various inverse dynamics formulations allow to implement whole-body controllers utilizing the dynamic equations of motion. A prominent example is the operational space control [6], that was extended to control the whole-body of humanoid robots [7][8]. An excellent survey on such methods is given in [9]. The authors of [10][11][12] have further extended this formulation proposing improved contact models. A comprehensive comparative analysis of the solutions adopted can be found in [13].

More recently, concepts from the computer graphics domain have emerged. Other than in inverse dynamic formulations, these methods represent unilateral constraints such as the contact and friction properties explicitly, and make use of quadratic programming techniques to solve for the joint torques. While they have been applied to problems in the computer graphics domain [14][15], the computational demands make it still hard to apply them to real-time control systems.

The solutions in the state-of-the-art have proven to be very effective in most of the scenarios tested, but they can be too restrictive when pushed to the limit ([7], Section 3.2.4). A typical example is a reaching task that has to be performed while maintaining the balance. In this case the highest priority is given to balancing. Usually, to guarantee that the robot can maintain its balance, the Zero-Moment Point (ZMP) [16] must remain at the center of the support polygon. This condition must continue to be satisfied when the hand reaches for the target. If the target is too far away the low priority task (reaching) is declared unfeasible and is not completed. A more flexible (or compliant) solution

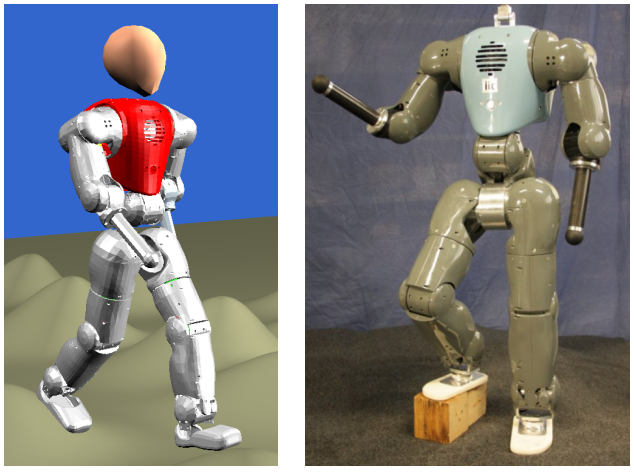

(a) (b)

Fig. 1. (a) The Robotran model of the COMAN robot (the head was added for a visualization purpose only), and (b) the 'light blue version' of the real COMAN

[1]Federico L. Moro, Nikos G. Tsagarakis, and Darwin G. Caldwell are with the Department of Advanced Robotics, Istituto Italiano di Tecnologia (IIT), via Morego 30, 16163, Genova, Italy federico.moro@iit.it

[2]Michael Gienger is with the Honda Research Institute (HRI) Europe, Carl-Legien-Straße 30, 63073 Offenbach/Main, Germany

[3]Ambarish Goswami is with the Honda Research Institute (HRI) USA, 425 National Avenue, Mountain View, CA 94043, USA

would be preferred: a small dislocation of the ZMP would not affect on the stability of the robot, and at the same time allows the reaching task to be successfully achieved.

Biological findings suggest that humans are often not as precise as robots, but tend instead to minimize the error from some preferred condition. It is uncommon to see a person maintain a perfect balance, but the balanced condition is undoubtedly a preferred one, and as the error grows the corrective action will become more evident. Moreover, reaching the preferred condition is also usually more important than the trajectories to reach it.

Following this philosophy, a technique based on a set of *attractors* is proposed in this paper. Every attractor is associated with a certain physical or derived measure (e.g., hand position, ZMP location, joint angular velocities, etc.), and works in parallel with other attractors generating joint torques that aim to modify the configuration of the robot so that the error in a target condition is minimized. For an end-effector attractor this is similar to virtual model control [17], or impedance control [18], or operational space control [6]. Intuitively it is easy to visualize an end-effector attractor as a (possibly non-linear) spring connecting the current end-effector position with the target position. The same idea can be extended to non physical variables, like the ZMP location, the centroidal angular momentum, or any other measured variable. A more precise definition of attractor will be provided in Section II.

There is no strict priority imposed between the tasks, but the importance of a variable with respect to the others is set by adjusting the weight of the attractors. The total torque applied to the joints is then a linear combination of the torques returned by each of the attractors. As long as the redundancy of the robot is sufficient to guarantee that optimality is reached by all the variables that are controlled, the attractors are not in conflict. In the situation described before, where the target hand position cannot be reached while maintaining the ZMP location exactly in the center of the support polygon, appropriate tuning of the weights becomes fundamental, so that the ZMP is allowed to move away from its optimal location by a certain amount, without affecting balance. In this way it is also possible to decide whether to be very conservative (attractors associated with balancing have a high weighting compared with other attractors), or be bolder (lowering the balance attractor weighting).

Balance is crucial in the design of a whole-body motion control system. As mentioned above, the most frequently adopted criterion is the well-known Zero-Moment Point [16], although, other criteria have been developed over the years [19][20]. Each of these proved to be very effective in a wide range of scenarios, but still they are only sufficient conditions for stability, and do not describe in full how humans maintain balance.

The WBMC system presented in this paper aims to be as general as possible, without being constrained to any specific condition (ground conditions, number of contacts with the ground, etc.). For this reason a more basic idea of equilibrium is considered, coming from the fundamentals of mechanics, and is adapted to fit the attractor-based structure of the system developed. As it will be explained in detail in Section II.B, this idea of equilibrium mainly deals with the *effort* of the robot and its *momenta*. The attractors operating to maintain the system close to the equilibrium are always active (balance is a permanent task), and together with other attractors that are also permanently (e.g., joint limits) or intermittently active (e.g., end-effector position) constitute the proposed attractor-based Whole-Body Motion Control (WBMC) system that will be presented in Section II.

The effectiveness of the proposed method was initially tested in simulation, and the are results reported in Section III. Once the reliability of the system was verified, the WBMC was used to torque-control the real COMAN humanoid robot (Figure 1) [21][22]. Results are reported as proof of concept in Section IV.

II. An Attractor-based Whole-Body Motion Control (WBMC) System

The WBMC system is a model-based, torque-control concept. It aims to control the simultaneous execution of several tasks, either permanent tasks (e.g., maintaining the balance), or temporary ones (e.g., reaching for a target with one hand). Each task is handled by an attractor that generates a torque to modify the robot's configuration toward a preferred one. In a more precise definition, an attractor f is a function having a vector of joint torques as output, which controls a certain quantity that is itself a function of $(q, \dot{q})$, i.e., the state of the system. This concept can be formulated as $\tau = f(g(q, \dot{q}))$. Particularly, the attractor f is the gradient of g with respect to either q or $\dot{q}$, hence $f = \nabla g$, where $\nabla g = \left[\frac{\partial g}{q_1} \cdots \frac{\partial g}{q_n}\right]$, e.g., the *MinEff* (Section II.B.1) or $\nabla g = \left[\frac{\partial g}{\dot{q}_1} \cdots \frac{\partial g}{\dot{q}_n}\right]$, e.g., the *MomCOM* (Section II.B.3). An attractor converges to a preferred configuration, locally minimizing g. A specific non-zero desired value $\overline{g}$ can also be imposed. In this case the attractor f will be the gradient of the error between g and $\overline{g}$, hence $f = \nabla(|g - \overline{g}|)$. This formulation describes the typical nature of an attractor. Small variations were applied in order to adapt this concept to best fit to the specific task, e.g., *MinEff* (Section II.B.1), *JLim* (Section II.C). The overall torque applied to the joints is the linear combination (Figure

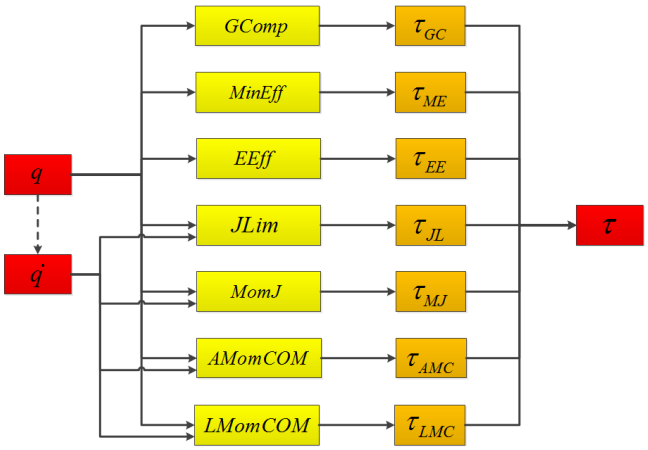

Fig. 2. The WBMC system is based on a set of *attractors*, each of which overtakes an imposed task. A linear combination of the torques generated by each attractors is applied to perform a whole-body motion. The modular structure of the proposed control system easily allows extensions.

2) of the torques generated by each attractor, plus a model-based gravity compensation that is described in Section II.A:

$$\tau = \tau_{GC} + \tau_{ME} + \tau_{MJ} + \tau_{LMC} + \tau_{AMC} + \tau_{JL} + \tau_{EE} + \cdots \quad (1)$$

The equilibrium is guaranteed by a set of four attractors that will be presented in Section III.B. A repulsion from the joint limits has also been developed, and will be described in Section III.C. Finally, position/force end-effector attractors will be presented in Section II.D. The modularity of the WBMC system ensures that other attractors can be easily implemented and added to the current ones (e.g., self collision avoidance).

It is also important to notice that each quantity associated to the attractors presented has a stand-alone value, that is independent from the entire WBMC system, and can be easily adapted to be included in other kinds of control systems.

A. Gravity Compensation for Free-Floating Base Robots

The WBMC system is based on a set of attractors that affect the robot configuration to minimize the error with respect to the task they are undertaking. They are all closed-loop controls, and for this reason their accuracy at steady-state is affected by constant disturbances, such as the gravitational effects. Therefore, a model-based gravity compensation is applied. This also allows to reduce the weight of the attractors.

It has turned out that the orthogonal decomposition method for gravity compensation of floating-base system [23][10] is advantageous due to its computational efficiency, and its open-loop character. In this approach contacts are considered as rigid, ideal constraints. Other works [14][15] propose more accurate models that also account for unilateral contacts with friction, however they are computationally still too expensive for hard real-time demands.

The COMAN robot was modeled as a 29-dofs system, 6 of which are unactuated and represent the floating base, while the other 23 are the actual joints of the robot. From the fundamental equation of the dynamics of a floating-base robot $M(q)\ddot{q} + C(q,\dot{q})\dot{q} + h(q) - J(q)^T F = S^T\tau$, neglecting the Coriolis term, and considering a static case, the following expression for gravity compensation can be derived [23][10]:

$$\tau_{GC}(q) = (N_c(q)S^T)^+ N_c(q) h(q) \quad (2)$$

where $N_c(q) = I - J(q)_c^+ J(q)_c$ is the null-space of the contacts with the environment, $J_c(q) = [J_{c1}(q)^T J_{c2}(q)^T \cdots J_{cm}(q)^T]^T$ is the concatenation of the Jacobians to the m contacts, $S = [0_{n\times 6} I_{n\times n}]$ is a selection matrix, with n being the number of active dofs, I is the identity matrix, and $^+$ is the pseudo-inverse operator. $P(q) = (N_c(q)S^T)^+ N_c(q)$ hence projects the $6+n$ torques returned by $h(q)$ into n torques to be applied by the active joints to compensate gravity. Whenever the system is subject to other external forces (e.g., the robot is holding an object), these can be compensated at the same time adding $J_{ext}(q)^T F_{ext}$ up to $h(q)$, and applying the same projection P.

In order to improve the computational efficiency, P can be reduced to a simpler form. Expanding the above pseudo-inverse, we get:

$$\begin{aligned} P &= ((N_c S^T)^T (N_c S^T))^{-1} (N_c S^T)^T N_c \\ &= (S N_c^T N_c S^T)^{-1} S N_c^T N_c \end{aligned}$$

Matrix N_c is idempotent: $N_c^T N_c = N_c$, and we get:

$$P = (S N_c S^T)^{-1} S N_c$$

If V_c is the orthonormal basis of the null-space, this expression can be further reduced by substituting N_c with $V_c V_c^T$, becoming:

$$\begin{aligned} P &= (S V_c V_c^T S^T)^+ S V_c V_c^T \\ &= ((S V_c)^+)^T (S V_c)^+ S V_c V_c^T \end{aligned} \quad (3)$$

In the case of $n = 23$ joints, as it is for the COMAN robot, with both feet on the ground, $N_c S^T$ in (2) is a (29×23) matrix, while SV_c in (3) is a (17×23) matrix. Since the pseudo-inverse is the most expensive operation among those used, Equation (3) is used to derive P, to reduce the computational time.

B. Equilibrium in a Multibody System

Balance plays a fundamental role in a whole-body control system. A controller that aims to coordinate the simultaneous execution of many tasks is always subject to the necessary condition that the robot must not fall while performing the desired actions. As already mentioned, ZMP [16] has been the most widely adopted method to guarantee balance over the last decades. This, and other methods [19][20] that were proposed more recently, have successfully accomplished this goal, but still represent only a sufficient condition for balancing, and do not capture the full complexity of human balance.

The system proposed in this paper aims to be as general as possible, and to not be constrained by any assumption, such as the number of contacts or the conditions of the terrain. For this reason a very basic definition of equilibrium coming from *Classical Mechanics* [24], page 113, was considered: *"A system of particles is in static equilibrium when all the particles of the system are at rest and the total force on each particle is permanently zero"*. This is a very strict definition, but describes clearly what a preferred condition for a system is (i.e., an *attractive* situation). In the case of a floating-base multi-body system the equilibrium refers both to the "inter-bodies" condition, and to the state of the system with respect to the inertial frame. The latter is well described by the CoM of the entire system. The safest and most controlled situation for a robot can be defined by the following terms:

1) the resultant force/torque acting on the system is zero, i.e., $F_{COM} = 0_{6\times 1}$, where F_{COM} is the vector of the spacial resultant force projected onto the CoM;
2) the "internal" torques generated by the external forces applied to the system are all zero, i.e., $\tau_j = 0_{n\times 1}$, where τ_j is the vector of the joint torques;
3) the system is at rest with respect to the world, i.e., $v_{COM} = 0_{6\times 1}$, where v_{COM} is the vector of the spacial velocities of the CoM;
4) the system is "internally" at rest, i.e., $v_j = 0_{n\times 1}$, where v_j is the vector of the n joint velocities.

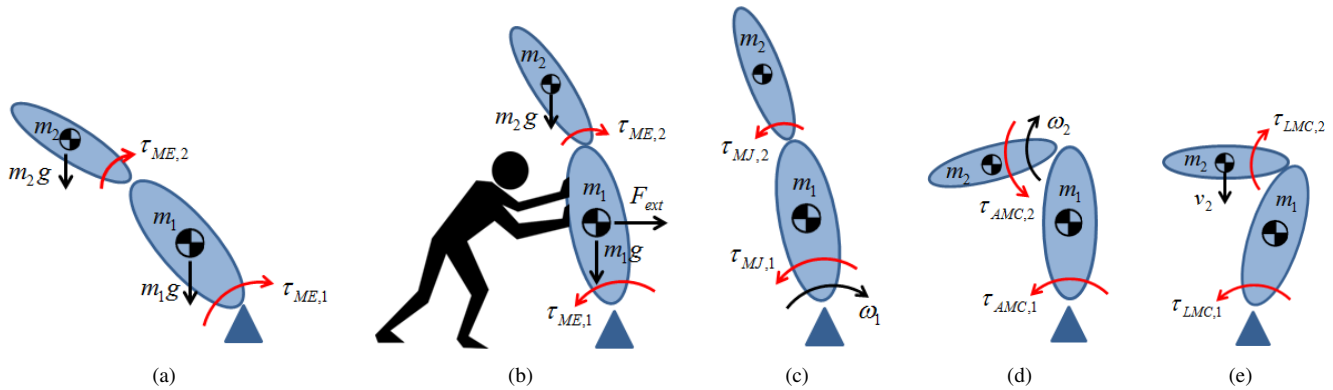

Fig. 3. The behavior of the WBMC system is not always easy to predict. The torques generated by the *MinEff* attractor in the case of a 2-link fixed-base robot, for instance, aim to bring the robot to a vertical position when gravity is the only external force acting on the robot (a). If another external force is applied (b), instead, the *MinEff* locally searches for a configuration that minimizes all external disturbances. In (c) the effect of the *MomJ* is shown. A positive torque in both joints is generated to compensate the effects of a negative angular velocity w_1 in joint 1. Similarly, the *AMomCOM* and *LMomCOM* generate a torque in all joints to reduce the velocity of the CoM caused, in this case, by w_2 and v_2, respectively.

If these conditions were permanently verified the robot would be substantially unable to act. The execution of a task requires these rules to be compliant: the robot is allowed to leave this preferred state, but never to get too far away from it. Loss of equilibrium means losing control of the robot: intuitively, if the controlled variables (velocities and forces) grow too large, the motors may not be powerful enough to generate the torques required to bring the system back to the equilibrium.

Based on these considerations, a set of attractors has been developed to guarantee that the robot always stays in the neighborhood of the equilibrium.

1) The Minimum Effort (MinEff) Attractor: Points 1 and 2 from the list in Section II.B are closely related to gravity (plus external forces) compensation. Whenever these two conditions are satisfied, $h(q) + J_{ext}(q)^T F_{ext}$ (contact reaction forces here are considered as external forces) will be equal to zero. This means that, if the system is also at rest (points 3 and 4), no torque needs to be applied by the motors to prevent the system from starting to move (both internally and with respect to the world frame). This also means that, as the external disturbances grow, a larger torque will be required to compensate for their effect. We define the robot effort as:

$$E = \tau_{GC}^T W \tau_{GC} \tag{4}$$

with τ_{GC} compensating for both gravity and any other external force, and where W is a weighting diagonal matrix that can be used to favor specific joints over the others. A minimization of the effort E is therefore beneficial not only, as is obvious, to reduce the energy consumption, but also to constrain the robot to a configuration that is closer to the equilibrium. To achieve this task, an attractor to the minimum effort (*MinEff*) was developed. Its expected behavior is the one of a gradient descent, where the gradient of the effort can be derived as:

$$\nabla E = \left[\frac{\partial E}{\partial q_1} \cdots \frac{\partial E}{\partial q_n} \right]^T \tag{5}$$

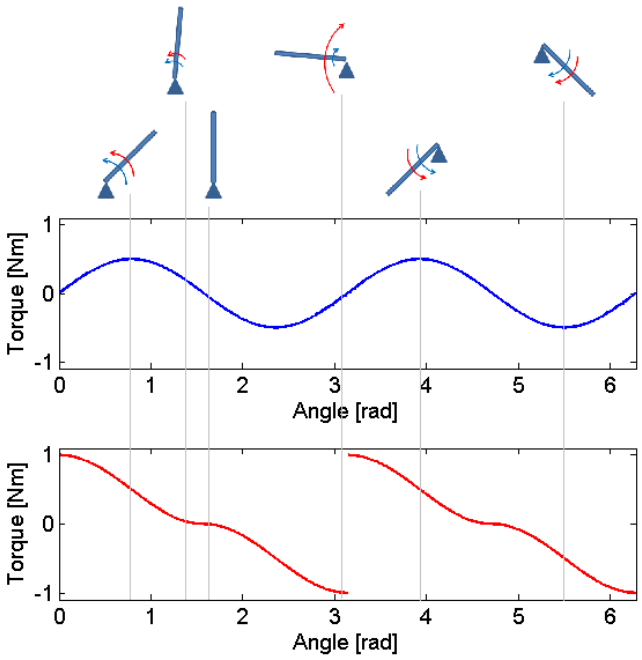

Fig. 4. The blue line represents the torque generated by the *MinEff* if $\tau_{ME} = -k_{ME}\nabla E$ in the case of a 1-link fixed-base system. The torque generated always has a correct direction, but when the link is almost horizontal (close to π in the example) the absolute value of the torque is small. A preferred behavior is depicted in the second graph (red line), where $\tau_{ME} = -k_{ME} sign(\nabla E)(\tau_{GC}\tau_{GC}^T)$. The direction is still coming from the gradient of effort E, but the absolute value monotonically increases as the angle diverges from the optimal configuration.

It can be verified that the behavior of an attractor of the kind $\tau_{ME} = -k_{ME}\nabla E$ can be further improved.

Applying it to a 1 link system attached to a fixed base by a rotational joint (Figure 4), with gravity and no other external disturbance, the link will be forced to move to a vertical position, either up or down ($\pm\pi/2$ if the zero is set at the link being horizontal). These two configurations are both minima in terms of effort, since link and gravity are parallel. As the angle changes from $\pm\pi/2$ to 0 (or $\pm\pi$), the effort E will

increase proportionally to the squared cosine of the angle. The gradient descent, hence, indicates the correct direction of movement. The absolute value of ∇E, though, is not monotonically increasing between $\pm\pi/2$ and 0 (or $\pm\pi$). If we consider the upper right quadrant, for instance, ∇E grows from zero, when the angle is $\pi/2$, to a maximum, when the angle is $\pi/4$, and then decreases again to zero, when the angle is 0 (the same applies to the other quadrants). If we set $\tau_{ME} \propto \nabla E$, then a small torque will be generated when the links is almost horizontal, while a bigger corrective torque is expected as the robot moves away from the equilibrium. A better formulation of the MinEff attractor is thus:

$$\tau_{ME} = -k_{ME} sign(\nabla E)(\tau_{GC}\tau_{GC}^T) \tag{6}$$

Two discontinuities are at 0° and 180°. Between these two angles (that represent the worst configurations in terms of effort) the behavior is similar to that of a quadratic spring with equilibrium at $\pm\pi/2$. Tuning the weight k_{ME} produces more conservative or more relaxed behaviors. It is important to notice that in more complex cases (many dofs, external forces, etc) the minimum effort configuration is not known as it is in the trivial example of the 1 link system (Figures 3(a) and 3(b)). The MinEff attractor performs a local search, and keeps modifying the configuration until a minimum is reached.

2) The Momentum at the Joints (MomJ) Attractor: One of the conditions for system equilibrium is that all joint velocities are at zero (point 4 from the list in Section II.B). Intuitively, this attractor is expected to behave as a damper. There are disadvantages, however, in simply setting this attractor as $\tau_{MJ} = -k_{MJ}\dot{q}$. The first is that each joint connects two subsystems that have an inertia that is typically different from the inertia seen by other joints. A unique k_{MJ} would not fit all cases. A specific k would have to be associated with each joint, and consequently this leads to a difficult tuning problem. The second problem to be considered is that in a multi-dofs system each joint is affected by the motion of the other joints to which it is connected: it would be not accurate to treat each joint as if it was independent from the others.

These considerations triggered the introduction of the concept of *momentum at a joint level*, defined as:

$$h_j = M\dot{q} \tag{7}$$

where M is the inertia matrix of the robot. The quantity h_j has been rarely exploited to control humanoid robots, although recently Orin et al. [25] have described its relation with other momenta.

The *MomJ* attractor is therefore defined as:

$$\tau_{MJ} = -k_{MJ}(M\dot{q}) \tag{8}$$

It depends on the joint velocities (Figure 3(c)), and attracts the system to a zero momentum at the joint level.

3) The Linear and Angular Momenta at the Center of Mass (MomCOM) Attractors: The *MinEff* and *MomJ* attractors control the quantities described at points 1,2, and 4 in Section II.B. Whenever the system is in (rigid, ideal) contact with the environment, if the joint velocities are zero, the CoM velocities are also zero (point 3). Even not considering the case of no contacts (though not so unusual, e.g., flight phase in running or jumping) having a direct control on the CoM velocities is fundamental for balance. There are situations where increasing the momentum at a certain specific joint can even be desirable, for instance to compensate for a large momentum in another joint, and reduce the overall momentum of the system (i.e., the CoM momentum). In the formulation proposed in [25], the linear and angular momenta are treated as a unique quantity (the *centroidal momentum*, a fundamental physical quantity for the control of a humanoid robot [4]). In the WBMC system, instead, it was decided to keep them separated with a dedicated attractor: this allows a priority to be imposed between the two. It can for instance be preferable to have a rigid control over the linear momentum, and be willing to be more relaxed on the angular momentum, or vice versa. The desired behavior can be accomplished by properly tuning the weight of the attractors.

The linear and the angular momenta about the CoM are calculated, respectively, as follows:

$$h_{g,lin} = \left(\sum_i m_i J_{T,COM,i}\right) \cdot \dot{q} \tag{9}$$

$$h_{g,ang} = \left(\sum_i m_i \tilde{r}_{COM,i} J_{T,COM,i} + I_i J_{R,i}\right) \cdot \dot{q} \tag{10}$$

where m_i is the mass of the i-th link, $J_{T,COM,i}$ is the translational part of the Jacobian to the CoM of the i-th link, $\tilde{r}_{COM,i}$ is the skew-symmetric form of $r_{COM,i}$, the relative position of the CoM of the i-th link, I_i is the inertia of the i-th link, and $J_{R,i}$ is the rotational part of the Jacobian to the end-effector of the i-th link.

In the case where the robot is standing in place the linear momentum is expected to be close to zero (Figure 3(e)) , while a non-zero reference can be set when the robot is, for instance, walking. If $\overline{v}$ is the vector of the desired gait velocity, the desired linear momentum can be indicated as $\overline{h}_{g,lin} = \overline{v}\sum_i m_i$. The *LMomCOM* attractor can therefore be defined as:

$$\tau_{LMC,i} = -k_{LMC}\frac{\partial(|h_{g,lin} - \overline{h}_{g,lin}|)}{\partial \dot{q}_i} \tag{11}$$

The preferred angular momentum, instead, is typically always zero (Figure 3(d)). The *AMomCOM* attractor, hence, can be expressed as:

$$\tau_{AMC,i} = -k_{SMC}\frac{\partial(|h_{g,ang}|)}{\partial \dot{q}_i} \tag{12}$$

Whenever a non-zero angular momentum reference is desired, this can be easily set by modifying Equation (12) accordingly.

C. Repulsion from the Joint Limits (JLim)

Maintaining equilibrium is not the only permanent task for a robot. It is vital to have accurate control on the motion of the robot near the joint limits to prevent the robot from damaging itself. A special attractor was designed to achieve

this purpose: unlike the other attractors, this is more the case of a *"repulsor"* from undesired configurations (i.e., joint limits). In order not to affect the behavior of the other attractors unnecessarily, a piecewise function was used, such that $\tau_{JL} = 0$ as long as the measured joint angle is not close to one of the limits. For each joint i, a positive (θ_i^+) and a negative (θ_i^-) threshold value are set. This functions both a safety margin $0.0 \leq \Delta \leq 0.5$, and the joint range $(q_i^+ - q_i^-)$. In detail, $\theta_i^+ = q_i^+ - \Delta(q_i^+ - q_i^-)$, and, similarly, $\theta_i^- = q_i^- + \Delta(q_i^+ - q_i^-)$. The joint range is hence divided into three parts by θ_i^- and θ_i^+: it works like a repulsive quadratic spring damper, when q_i exceeds the thresholds, and has no effect otherwise. If $q_i < \theta_i^-$, then:

$$\tau_{JL,i} = k_{JL,S} \left(\frac{q_i - \theta_i^-}{q_i^- - \theta_i^-} \right)^2 - k_{JL,D}(\dot{q}_i) \qquad (13)$$

When, instead, $\theta_i^- \leq q_i \leq \theta_i^+$:

$$\tau_{JL,i} = 0 \qquad (14)$$

Last, if $q_i > \theta_i^+$, then:

$$\tau_{JL,i} = -k_{JL,S} \left(\frac{q_i - \theta_i^+}{q_i^+ - \theta_i^+} \right)^2 - k_{JL,D}(\dot{q}_i) \qquad (15)$$

To avoid a "sticky" effect, $\tau_{JL,i}$ in Equation (13) always has to be greater than or equal to zero, while in Equation (15) it has to be less than or equal to zero.

D. The Position/Force End-Effector (EEff) Attractors

The end-effector attractors work like in the operational space formulation [6] for underactuated systems [7][8]. An end-effector force is generated from the error in the end-effector position and velocity (linear spring and damper): $F_{EE} = k_{EE,S}(\bar{x}_{EE} - x_{EE}) + k_{EE,D}(\dot{\bar{x}}_{EE} - \dot{x}_{EE})$. The joint torques are derived from F_{EE} through the end-effector Jacobian J_{EE}, and the projection P from Section II.A:

$$\tau_{EE} = P(J_{EE}^T F_{EE}) \qquad (16)$$

This formulation can be easily modified to directly track a reference force instead of a position, for instance when a well determined force has to be applied in a contact.

III. Results in Simulation

The validity of the proposed approach was first tested in simulation. The 29-dofs model of COMAN was developed in Robotran [26], including the information on the full dynamics of the robot obtained from the CAD of the real prototype (Figure 1(a)). The focus of the tests was on the interaction between the attractors responsible for the equilibrium, i.e., *MinEff*, *MomJ*, *MomCOM*. The following example shows the behavior of the robot when subject to the effect of these attractors, together with the gravity compensation term, and the repulsion from the *JLim*:

$$\tau = \tau_{GC} + \tau_{ME} + \tau_{MJ} + \tau_{LMC} + \tau_{AMC} + \tau_{JL} \qquad (17)$$

The weights of the attractors were adjusted to match the expected behavior of the system. The simulation starts with COMAN standing in place with bent knees, i.e., in a non minimum effort configuration. All initial joint velocities are

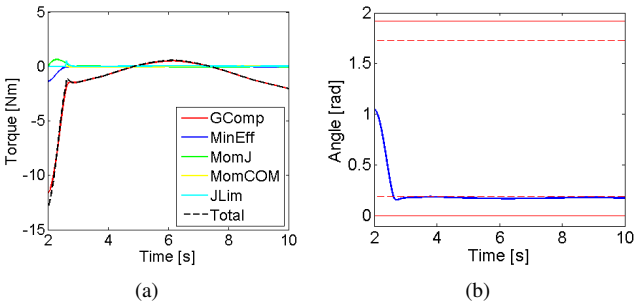

Fig. 5. (a) Right knee torques generated by the attractors. The *MinEff* contributes to straighten the knee to a configuration that requires a torque that is significantly smaller to compensate the effects of gravity. The *MomJ* behaves like a damping on the joint velocity, while the effects of the *MomCOM* are negligible in this case. The *JLim*, instead, produces a torque that prevents the joint limit to be reached. This is clearer in (b), where the knee angle is shown. It can be noticed that the knee straightening happens in less than 1 second, and that the joint limit is never reached. This reduces the risk to damage the robot itself.

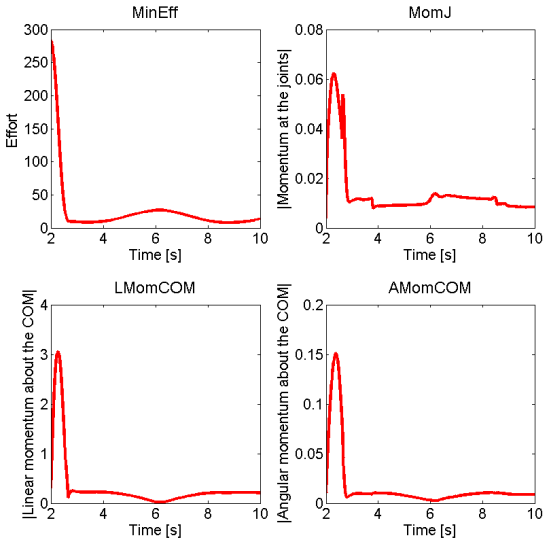

Fig. 6. The four graphs above show how the values of the measures that are controlled in the simulation change over time. Particularly, the effort reduces to a value that is ten times smaller than the initial. The momenta, instead, initially grow as the robot starts moving, and then reduce again to small values with negligible oscillations.

set to zero. The WBMC starts controlling all joints of the robot at second 2. The combined effect of the attractors results in a stable straightening of the legs toward a balanced, minimum effort configuration in about 1 second. Figure 5 shows the results for the right knee. Particularly, in Figure 5(a) the torques generated by the different attractors are reported. It can be noticed that the torque required for compensating gravity reduces from about $12Nm$ (in absolute value) to less than $2Nm$. This occurs as the torque generated by the *MinEff* (blue line) contributes to the straightening of the legs. The *MomJ* (green line) generates a torque with sign opposite to the velocity, acting as a damping. The *MomCOM* (yellow line) have a negligible effect in this case. It can also be noted that a small peak of torque is generated by the *JLim* (light blue) as the knee approached its limit. This is clearer in Figure 5(b), that shows the trajectory of the knee joint angle: from about $1rad$ the knees reaches fast the threshold of

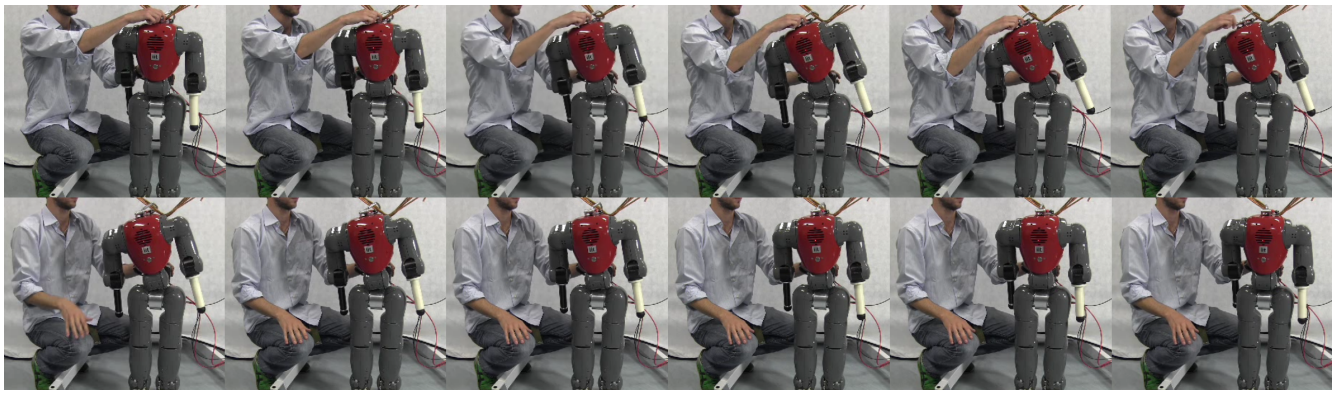

Fig. 7. Snapshots from the video of the experimental validation of the WBMC with the COMAN robot (taken at $2Hz$). In this instance the robot configuration is perturbed by forcing the waist roll joint to change its angle. As the robot is released the *MinEff* brings the robot back to a vertical, minimum effort configuration. The resulting motion is damped by the *MomJ* attractor, that prevents the velocity to grow uncontrolled.

approximatively $0.19rad$. The knee is not allowed to stretch much more to avoid the reaching of the joint limit, i.e., $0rad$. The knee angle stabilizes around $0.18rad$ with negligible oscillations.

The behavior of the overall system can be appreciated from Figure 6, that shows how the controlled measures change as the WBMC affects the configuration of the robot. The effort of the robot significantly reduces to a value that is 10 times smaller than the initial. The momenta, instead, initially grow as the robot starts moving, and then reduce again to very small values. The small peak in the *MomJ* graph around second 3 is caused by the *JLim* repulsion.

IV. Tests with the COMAN Robot

As the reliability of the WBMC system was verified in simulation, some preliminary tests were performed with the real COMAN robot (Figure 1(b)). The reference torques generated by the WBMC were tracked in each joint by a PI torque control loop at $1kHz$. Few are the examples of torque controlled humanoid robots in the state-of-the-art. Among these, a successful instance is [27]. In this first test, the waist pitch and roll joints are controlled by the WBMC, the shoulder pitch and roll of the right arm are zero-torque controlled, and all other joints are controlled in position (Figure 7 shows some snapshots from the video of the experiments with COMAN). In this simplified scenario the effect of the *MomCOM* is not significant: for this reason only the gravity compensation term, the *MinEff* attractor, and the *MomJ* attractor are activated. The weights of the attractors are set basing on the experience in simulation.

$$\tau = \tau_{GC} + \tau_{ME} + \tau_{MJ} \tag{18}$$

This experiment starts with COMAN in the minimum effort configuration, with zero joint velocities. An external disturbance perturbs the equilibrium, with the WBMC opposing to this imposed displacement. At release, COMAN moves back to its preferred configuration. Figure 8 shows the results obtained for the pitch waist joint. Between $0s$ and $1s$ the robot is pushed forward. As a consequence, the torque required to compensate the effects of gravity grow to about $4Nm$. The *MinEff* grows as well, as it tries to bring the robot back. Also the *MomJ* is pushing back, in a direction

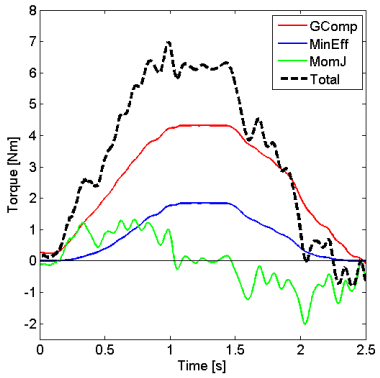

Fig. 8. As the configuration of the waist pitch joint is perturbed, the torque required to compensate gravity grows to about $4nM$. Also the torque generated by the *MinEff* increases, as it attempts to bring back to robot to its preferred configuration. The velocity of the motion also produced a damping torque by means of the *MomJ*. This drops down to zero when the robot is maintained in the position. As the robot is released, instead, the *MinEff* brings it back to the minimum effort configuration. To verify this, it can be noticed that the torque generated by the gravity compensation term reduces as well. The torque generated by the *MomJ* has a negative sign in this phase, since the joint velocity is now positive.

that is the opposite of the joint velocity. The robot is kept in a bent configuration for $0.5s$ (between $1s$ and $1.5s$): both gravity compensation and *MinEff* remain constant, while the torque generated by *MomJ* drops down to zero, since there is no joint velocity. The robot is then released, and the *MinEff* brings it back to the preferred configuration in $1s$ (between $1.5s$ and $2.5s$). As an effect, also the gravity compensation decreases. In this last phase, instead, the *MomJ* is pushing forward, behaving as a damping on the joint velocity.

It can be noticed that the torques generated to compensate gravity, and by the *MinEff* are very smooth. The *MomJ*, instead, is more noisy: this is because this measure depends on the joint velocity, that is derived numerically from the joint angle.

V. Conclusions

A novel approach to the whole-body control of humanoid robots is proposed. This new method aims to be more flexible when compared to the other whole-body control systems

found in the literature that are based on inverse dynamics. This compliant behavior was achieved by using so-called *attractors*: unitary modules that are associated to each task. Balance is guaranteed by a set of attractors that are designed to satisfy a basic definition of equilibrium coming from classical mechanics. The validity of the proposed method is tested both in simulation and on the real COMAN robot. The main contributions of this work can be summarized as:

- introduction of the *attractors*: unitary tools that affect the configuration of the robot driving it towards a more preferred one. Each controlled task is associated with an attractor;
- derivation of a computationally efficient gravity compensation for floating-base systems;
- use of a basic definition of equilibrium to verify the balance of the robot, based on the effort and on the momenta;
- novel use of the effort of the robot as an indicator of equilibrium;
- novel use of the momentum at the joints to control a humanoid robot;
- design of a complete attractor-based Whole-Body Motion Control (WBMC) system;
- validation on both simulation and with a real torque-controlled robot, the compliant humanoid COMAN.

The results presented confirm the effectiveness of the proposed novel approach. Further tests with COMAN are scheduled, to apply the WBMC system to the entire robot in more challenging tasks. The modular structure of the proposed control system easily allows extensions: a stepping/walking strategy will be integrated in the near future. A systematic analysis of the interaction among attractors will also be performed, with the aim to establish a repeatable procedure for tuning the weight of the attractors. The system was also proven to be sufficiently robust to the unavoidable model errors, while the main limitation is the strong dependence on the quality of the torque tracking, which is highly affected by the accuracy of the sensors. The concepts presented are not limited to humanoid robots, but transferable to multi-legged robots, such as quadrupeds or hexapods.

ACKNOLEDGMENTS

Federico L. Moro warmly thanks Jody A. Saglia and Andrea Del Prete for the helpful discussions on the topics presented in this paper, and Alessio Margan for the work done to implement and optimize the C-code of the WBMC system.

REFERENCES

[1] Y. P. Ivanenko, G. Cappellini, N. Dominici, R. E. Poppele, and F. Lacquaniti, "Coordination of locomotion with voluntary movements in humans," *The Journal of Neuroscience*, vol. 25, no. 31, pp. 7238–7253, 2005.

[2] F. L. Moro, N. G. Tsagarakis, and D. G. Caldwell, "On the Kinematic Motion Primitives (kMPs): Theory and Application," *Frontiers in Neurorobotics*, vol. 6, no. 10, pp. 1–18, 2012.

[3] Y. Nakamura, *Advanced Robotics: Redundancy and Optimization.* Addison-Wesley Publishing Company, 1991.

[4] S. Kajita, F. Kanehiro, K. Kaneko, K. Fujiwara, K. Harada, K. Yokoi, and H. Hirukawa, "Resolved momentum control: humanoid motion planning based on the linear and angular momentum," in *IEEE/RSJ International Conference on Intelligent Robots and Systems*, (Las Vegas, NV, USA), 2003.

[5] M. Gienger, M. Toussaint, and C. Goerick, "Whole-body motion planning - building blocks for intelligent systems," in *Motion Planning for Humanoid Robots* (K. Harada, E. Yoshida, and K. Yokoi, eds.), Springer, 2010.

[6] O. Khatib, "A unified approach for motion and force control of robot manipulators: The operational space formulation," *IEEE Journal of Robotics and Automation*, vol. 3, no. 1, pp. 43–53, 1987.

[7] L. Sentis, *Synthesis and Control of Whole-Body Behavior in Humanoid Systems*. PhD thesis, Stanford University, CA, USA, 2007.

[8] L. Sentis, "Compliant control of whole-body multi-contact behaviors in humanoid robots," in *Motion Planning for Humanoid Robots* (K. Harada, E. Yoshida, and K. Yokoi, eds.), Springer, 2010.

[9] J. Peters, M. Mistry, F. Udwadia, J. Nakanishi, and S. Schaal, "A unifying framework for robot control with redundant DOFs," *Autonomous Robots*, vol. 24, no. 1, pp. 1–12, 2008.

[10] L. Righetti, J. Buchli, M. Mistry, and S. Schaal, "Inverse dynamics control of floating-base robots with external constraints: A unified view," in *IEEE International Conference on Robotics and Automation*, (Shanghai, China), 2011.

[11] M. Mistry and L. Righetti, "Operational space control of constrained and underactuated systems," in *Robotics: Science and Systems Conference*, (Los Angeles, CA, USA), 2011.

[12] L. Saab, O. E. Ramos, F. Keith, N. Mansard, P. Soueres, and J.-Y. Fourquet, "Dynamic whole-body motion generation under rigid contacts and other unilateral constraints," *IEEE Transactions on Robotics*, vol. 29, no. 2, pp. 346–362, 2013.

[13] A. Del Prete, *Control of Contact Forces using Whole-Body Force and Tactile Sensors: Theory and Implementation on the iCub Humanoid Robot*. PhD thesis, Istituto Italiano di Tecnologia, Italy, 2013.

[14] Y. Abe, M. da Silva, and J. Popović, "Multiobjective control with frictional contacts," in *ACM SIGGRAPH/Eurographics symposium on Computer animation*, (San Diego, California), 2007.

[15] P. M. Wensing and D. E. Orin, "Generation of dynamic humanoid behaviors through task-space control with conic optimization," in *IEEE International Conference on Robotics and Automation*, (Karlsruhe, Germany), 2013.

[16] M. Vukobratovic and B. Borovac, "Zero-moment point - thirty five years of its life," *International Journal of Humanoid Robotics*, vol. 1, no. 1, pp. 153–173, 2004.

[17] J. Pratt, C.-M. Chew, A. Torres, P. Dilworth, and G. Pratt, "Virtual Model Control: An Intuitive Approach for Bipedal Locomotion," *The International Journal of Robotics Research*, vol. 20, no. 2, pp. 129–143, 2001.

[18] N. Hogan, "Impedance control: An approach to manipulation: Part I - theory," *Journal of Dynamic Systems, Measurement, and Control*, vol. 107, pp. 1–24, 1985.

[19] M. B. Popovic, A. Goswami, and H. Herr, "Ground Reference Points in Legged Locomotion: Definitions, Biological Trajectories and Control Implications," *The International Journal of Robotics Research*, vol. 24, no. 12, pp. 1013–1032, 2005.

[20] A. Goswami and V. Kallem, "Rate of change of angular momentum and balance maintenance of biped robots," in *IEEE International Conference on Robotics and Automation*, (New Orleans, LA, USA), 2004.

[21] N. G. Tsagarakis, Z. Li, J. Saglia, and D. G. Caldwell, "The design of the lower body of the compliant humanoid robot ccub," in *IEEE International Conference on Robotics and Automation*, (Shanghai, China), 2011.

[22] F. L. Moro, N. G. Tsagarakis, and D. G. Caldwell, "A human-like walking for the COmpliant huMANoid COMAN based on CoM trajectory reconstruction from kinematic Motion Primitives," in *IEEE-RAS International Conference on Humanoid Robots*, (Bled, Slovenia), 2011.

[23] M. Mistry, J. Buchli, and S. Schaal, "Inverse dynamics control of floating base systems using orthogonal decomposition," in *IEEE International Conference on Robotics and Automation*, (Anchorage, AK, USA), 2010.

[24] H. C. Corben and P. Stehle, *Classical Mechanics*. Courier Dover Publications, 2nd ed., 1960.

[25] D. E. Orin, A. Goswami, and S.-H. Lee, "Centroidal Dynamics of a Humanoid Robot," *Autonomous Robots*, 2013. (online).

[26] H. Dallali, M. Mosadeghzad, G. Medrano-Cerda, N. Docquier, P. Kormushev, N. Tsagarakis, Z. Li, and D. Caldwell, "Development of a dynamic simulator for a compliant humanoid robot based on a symbolic multibody approach," in *International Conference on Mechatronics*, (Vicenza, Italy), 2013.

[27] B. J. Stephens and C. G. Atkeson, "Dynamic balance force control for compliant humanoid robots," in *IEEE/RSJ International Conference on Intelligent Robots and Systems*, (Taipei, Taiwan), 2010.